structural types. This work is underway in our and other laboratories.

Acknowledgment. We thank the National Science Foundation (CHE 81-04997) and the National Institutes of Health (GM-30147) for support of this work and Prof. P. L. Polavarapu for use of his LMO program. T.A.K. thanks Prof. K. L. Kompa and the Max-Planck-Institut für Quantenoptik for hospitality during the time when this paper was being written and the Fulbright Foundation for support.

Registry No. *trans*-1,2-Dideuteriocyclobutane, 75156-31-9.

Relative Electron Affinities of Substituted Benzophenones, Nitrobenzenes, and Quinones

Elaine K. Fukuda and Robert T. McIver, Jr.*

Contribution from the Department of Chemistry, University of California, Irvine, California 92717. *Received June 20, 1984*

Abstract: The relative electron affinities of 53 molecules have been determined by measuring equilibrium constants for gas-phase electron-transfer reactions of the general type $A^{-}\cdot + B = B^{-}\cdot + A$. A pulsed ion cyclotron resonance (ICR) spectrometer was utilized to generate, store, and detect molecular anion radicals at pressures below 1×10^{-5} torr. The ions were generated by electron capture and stored for several hundred milliseconds in a one-region ICR analyzer cell. A scale of relative electron affinities has been constructed by using the method of multiple overlaps. Substituent effects on the electron affinities of various nitrobenzenes, benzophenones, and quinones are discussed.

Chemical reactions involving negative ions are ubiquitous. For example, the primary source of visible light from the sun results from radiative electron attachment to hydrogen atoms.[1] In the earth's atmosphere, negative ions such as O^-, Cl^-, and NO_2^- play an important role in the chemistry of the ionsphere.[2] Many reactions in solution are being interpreted in terms of the single-electron-transfer (SET) mechanism.[3] And it is well-known that such biologically important processes as photosynthesis and oxidative phosphorylation involve electron-transfer reactions.

One of the fundamental properties of a gaseous negative ion is the lowest energy required to remove an electron. This energy is called the electron affinity (EA) and is equal to ΔE for the process

$$A^- = A + e^- \quad (1)$$

where both the ion and neutral are gaseous species in their ground electronic, vibrational, and rotational states, and the electron has zero kinetic and potential energy. The quantity EA is positive if a stable negative ion exists.

Many experimental methods have been developed for measuring electron affinities.[4] Photodetachment and photoelectron spectroscopy (PES) are optical methods which study the reaction

$$A^- + h\nu \rightarrow A + e^- \quad (2)$$

In the photodetachment experiment, ion abundance is monitored as a function of varying wavelength to determine the threshold for photodetachment,[5,6] while in photoelectron spectroscopy a fixed frequency light source intersects a beam of negative ions and the resultant photoelectrons are energy-analyzed.[7]

Another approach involves observing the occurrence of ion–molecule charge-transfer reactions such as

$$SH^- + NO_2 \rightarrow NO_2^- + SH \quad (3)$$

Since this is a fast reaction at thermal energies, it is safe to conclude that the $EA(NO_2)$ is greater than EA(SH). Exothermic charge-transfer reactions have been studied with flowing afterglow systems[8] and ion cyclotron resonance spectrometers.[9,10] Another approach involves the use of tandem mass spectrometers[11] and alkali atom beam instruments[12,13] to study the translational energy dependence for endothermic electron-transfer reactions.

The gas-phase acidity scale has been used to calculate the electron affinities of several radicals.[14–16] Equilibrium constants for reactions of the type

$$F^- + AH = A^- + HF \quad (4)$$

(1) Wildt, R. *Astrophys. J.* **1939**, *89*, 295.
(2) Ferguson, E. E.; Fehsenfeld, F. C.; Albritton, D. L. In "Gas Phase Ion Chemistry"; Bowers, M. T., Ed.; Academic Press: 1979; Vol. 1, Chapter 2.
(3) For example, see: (a) Amatore, C.; Pinson, J.; Saveant, J.-M.; Thiebalt, A. *J. Am. Chem. Soc.* **1981**, *103*, 6930. (b) Guthrie, R. D.; Cho, N. S. *J. Am. Chem. Soc.* **1979**, *101*, 4698. (c) Klinger, R. J.; Mochida, K.; Kochi, J. K. *J. Am. Chem. Soc.* **1979**, *101*, 6626.
(4) For recent reviews of electron affinities see: (a) Janousek, B. K.; Brauman, J. I. In "Gas Phase Ion Chemistry"; Bowers, M. T., Ed.; Academic Press: New York, 1979; Vol. 2, p 53. (b) Corderman, R. R.; Lineberger, W. C. *Annu. Rev. Phys. Chem.* **1979**, *30*, 347.
(5) Branscomb, L. M. In "Atomic and Molecular Processes"; Bates, D. R., Ed.; Academic Press: New York, 1962; p 100.
(6) Smyth, K. C.; Brauman, J. I. *J. Chem. Phys.* **1972**, *56*, 1132.
(7) Lineberger, W. C. In "Chemical and Biochemical Applications of Lasers"; Moore, C. B., Ed.; Academic Press: New York, 1974; Vol. 1, p 71.
(8) Dunkin, D. B.; Fehsenfeld, F. C.; Ferguson, E. E. *Chem. Phys. Lett.* **1972**, *15*, 257.
(9) Fukuda, E. K.; McIver, R. T., Jr. *J. Chem. Phys.* **1982**, *77*, 4942.
(10) Rains, L. J.; Moore, H. W.; McIver, R. T., Jr. *J. Chem. Phys.* **1978**, *68*, 3309.
(11) Lifshitz, C.; Tiernan, T. O.; Hughes, B. M. *J. Chem. Phys.* **1973**, *59*, 3182.
(12) (a) Nalley, S. J.; Compton, R. N. *Chem. Phys. Lett.* **1971**, *9*, 529. (b) Nalley, S. J.; Compton, R. N.; Schweinler, H. C.; Anderson, V. E. *J. Chem. Phys.* **1973**, *59*, 4125.
(13) Leffert, C. B.; Jackson, W. M.; Rothe, E. W.; Fenstermaker, R. W. *Rev. Sci. Instrum.* **1972**, *43*, 917; (b) Leffert, C. B.; Jackson, W. M.; Rothe, E. W. *J. Chem. Phys.* **1973**, *58*, 5801.
(14) Bartmess, J. E.; Scott, J. A.; McIver, R. T., Jr. *J. Am. Chem. Soc.* **1979**, *101*, 6046.
(15) Bartmess, J. E.; Scott, J. A.; McIver, R. T., Jr. *J. Am. Chem. Soc.* **1979**, *101*, 6056.
(16) Bartmess, J. E.; McIver, R. T., Jr. In "Gas Phase Ion Chemistry"; Bowers, M. T., Ed.; Academic Press: New York, 1979; Vol. 2, Chapter 11.

0002-7863/85/1507-2291$01.50/0

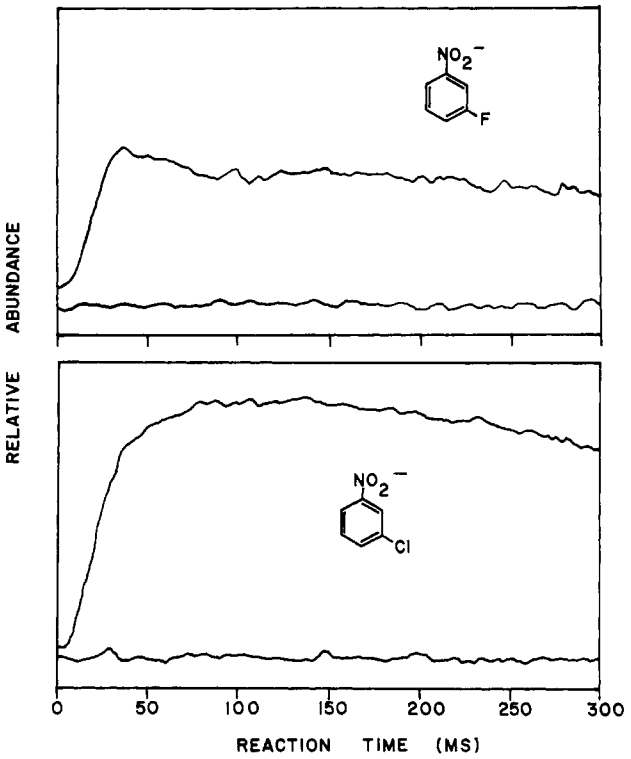

Figure 1. Pulsed ICR time plots for m/z 141$^-$ and m/z 157$^-$ in a mixture of *m*-fluoronitrobenzene and *m*-chloronitrobenzene.

measure the gas-phase acidity (proton donor ability) of AH relative to hydrogen fluoride. Knowing the heats of formation of F^- and HF, the enthalpy change $\Delta H_{acid}°$ can be calculated for the process

$$AH = A^- + H^+ \quad (5)$$

When a simple thermodynamic cycle is used, $\Delta H_{acid}°$ can be written as

$$\Delta H_{acid}° = DH°(A–H) + IP(H) - EA(A) \quad (6)$$

where DH°(A–H) is the homolytic A–H bond strength. IP(H) is the ionization potential of hydrogen (313.6 kcal/mol) and EA(A) is the adiabatic electron affinity of the radical A.

In this paper we report pulsed ion cyclotron resonance (ICR) measurements of equilibrium constants for gas-phase electron-transfer reactions of the general type

$$A^{-}\cdot + B = B^{-}\cdot + A \quad (7)$$

where A and B are a wide variety of substituted benzophenones, nitrobenzenes, and quinones. Some preliminary results have been reported previously.[17,18] The equilibrium constants for these reactions are closely related to the relative electron affinities of the molecules and can be used to construct a scale of relative gas-phase electron affinities. The scale covers a range of almost 2 eV. Substituent effects on the electron affinities are discussed, and the relative electron affinities determined by the ICR method are compared with those measured by other methods.

Experimental Section

The electron affinity measurements reported in this paper were performed with a pulsed ion cyclotron resonance (ICR) mass spectrometer which was constructed in our laboratory at the University of California at Irvine. The pulsed ICR technique utilizes the cyclotron resonance principle for mass analysis of gaseous ions stored in a one-region trapped ICR cell. A pulsed mode of operation is used for ion formation, trapping, double resonance irradiation, and mass analysis. At a typical operating pressure of 5×10^{-6} torr, ions are stored for about 1 s by a uniform magnetic field of 1.3 T and a weak electric field (0.5 V/cm). The ions suffer on the order of a hundred ion–neutral collisions while stored in the ICR cell. This is generally sufficient to thermalize them to the temperature of the neutral gas. Many of the experimental techniques utilized for this study are similar to those used for construction of the gas-phase acidity scale[14–16] and the proton affinity scale.[19–21]

Scheme I

$$A + e^- \rightleftharpoons [A^{-}\cdot]^* \longrightarrow A^{-}\cdot + h\nu \quad (8)$$
$$[A^{-}\cdot]^* \xrightarrow{M} A^{-}\cdot + M^*$$
$$B + e^- \rightleftharpoons [B^{-}\cdot]^* \longrightarrow B^{-}\cdot + h\nu \quad (9)$$
$$[B^{-}\cdot]^* \xrightarrow{M} B^{-}\cdot + M^*$$
$$A^{-}\cdot + B \rightleftharpoons B^{-}\cdot + A \quad (10)$$
$$A^{-}\cdot + M \longrightarrow \text{ion loss} \quad (11)$$
$$B^{-}\cdot + M \longrightarrow \text{ion loss} \quad (12)$$

Scheme I shows the sequence of reactions that occurs in a pulsed ICR study of an electron-transfer equilibrium. An experiment is initiated by a 10-ms pulse of a low-energy electron beam (0.5 eV) through the ICR cell. Inelastically scattered electrons are trapped in the cell and captured by the neutral reactants to form excited negative ion radicals which can either autodetach an electron or be stabilized by spontaneous emission and collisions with a buffer gas M.[10,22] Negative ion radicals that are difficult to observe in conventional mass spectrometer ion sources can be easily produced in a trapped ICR cell because the autodetached electrons are trapped by the electric fields of the cell and recaptured to produce negative ions that are ultimately stabilized. Reversible electron transfer, reaction 10, is another important mechanism for thermalizing the ions. After a sufficiently long delay time, typically 300 ms, the ions become thermalized and an equilibrium constant K can be calculated where

$$K = \frac{[B^{-}\cdot]\,[A]}{[A^{-}\cdot]\,[B]} \quad (13)$$

The relative abundances of $A^{-}\cdot$ and $B^{-}\cdot$ are determined with a capacitance bridge detector, and the pressures of neutral species are measured with a Bayard-Alpert ionization gauge that has been calibrated with a Baratron-type 145-AHS capacitance manometer.[23]

Electron-transfer reactions involving substituted benzophenones were slower than the others we studied. As a result, the equilibrium constant measurements are more susceptible to ion loss processes which cause the ions to diffuse gradually out of the ICR cell. This problem was minimized by working at constant magnetic field strength so that the rates of ion loss from the ICR cell would be comparable.[24] Another potential cause for concern is the occurrence of alternate reaction channels which perturb the equilibria. Fortunately, this did not cause difficulties with the systems reported here because electron transfer was the dominant reaction channel observed.

Ion cyclotron double-resonance experiments were done on each reported equilibrium reaction to check that the electron-transfer reactions were sufficiently fast compared to the time scale of the experiment. Double-resonance experiments were performed by scanning the magnetic field across the resonance for an ion, first with the double-resonance rf turned off and then with it turned on. This procedure was used to avoid spurious double-resonance effects caused by shifts in the position of the resonance.[25]

Many compounds investigated in this study are high boiling liquids or solids. It was necessary, therefore, to operate the inlet system and the ICR analyzer at elevated temperatures. The inlet system is constructed of 304 stainless steel tubing, all-metal bellows-sealed valves (Hoke Model 4213Q6Y), and variable leak valves (Varian Type 951-5106). Solid samples were placed in individual stainless steel cups which were connected to the inlet system by using Cajon 6-VCR flanges. During an experiment, the inlet system and the ICR analyzer were warmed to 80–85 °C with resistance heating tapes. Temperatures were measured with

(17) Fukuda, E. K.; McIver, R. T. Jr. *J. Phys. Chem.* **1983**, *87*, 2993.
(18) McIver, R. T., Jr.; Fukuda, E. K. In "Ion Cyclotron Resonance Spectrometry II"; Hartmann, H., Wanzcek, K. P., Eds.; Springer-Verlag: New York, 1982; p 164.
(19) Wolf, J. F.; Staley, R. H.; Koppel, I.; Taagepera, M.; McIver, R. T., Jr.; Beauchamp, J. L.; Taft, R. W. *J. Am. Chem. Soc.* **1977**, *99*, 5417.
(20) Aue, D. H.; Bower, M. T. In "Gas Phase Ion Chemistry"; Bowers, M. T., Ed.; Academic Press: New York, 1979; Vol. 2, Chapter 9.
(21) Taft, R. W. In "Proton Transfer Reactions"; Caldin, E. F., Gold, V., Ed.; Wiley-Halsted: New York, 1975; p 31.
(22) Foster, M. S.; Beauchamp, J. L. *Chem. Phys. Lett.* **1975**, *31*, 482.
(23) McIver, R. T., Jr.; Ledford, E. B., Jr.; Hunter, R. L. *J. Chem. Phys.* **1980**, *72*, 2535.
(24) Francl, T. J.; Fukuda, E. K.; McIver, R. T., Jr. *Int. J. Mass Spectrom. Ion Phys.* **1983**, *50*, 151.
(25) DeFrees, D. J.; Hehre, W. J.; McIver, R. T., Jr.; McDaniel, D. H. *J. Phys. Chem.* **1979**, *83*, 232.

copper–constantan thermocouples attached to the ICR cell and to the wall of the analyzer. Normally there was a gradient of only a few degrees if the cell filament current was kept below 2 A. For the purposes of calculating free energy changes, the average of the two readings taken at the ICR cell was taken. The analyzer system was baked at 150 °C overnight and pumped by an 8 L/s ion pump to achieve base pressures in the low 10^{-8}-torr range.

Most compounds were obtained commercially and were checked for purity by their positive ion and negative ion mass spectra in the ICR instrument itself. Any needed purifications were effected by the appropriate distillation, recrystallization, or sublimation procedures. Removing water from the benzophenone samples was a problem. Following recrystallization, molecular sieve beads (MCB Type 3 Å) were added to the sample cup as it was put on the inlet system, and the ICR spectrum was monitored until the water signal was no longer detected. Each liquid or gas sample was subjected to freeze–pump–thaw cycles on the ICR inlet system to remove air. The inlet ports containing solid samples were degassed to the diffusion-pumped foreline to remove trapped air.

Results

A typical pulsed ICR time plot of ion abundance vs. reaction time is shown in Figure 1 for an electron-transfer reaction between *m*-chloronitrobenzene and *m*-fluoronitrobenzene. The *m*-chloronitrobenzene sample was first added to the ICR analyzer system until its pressure had stabilized at 1.3×10^{-6} torr. Then *m*-fluoronitrobenzene was added to a partial pressure of 2.5×10^{-6} torr. Figure 1 shows that under these conditions the molecular anion of each compound forms rapidly during the first 40 ms. Subsequently, m/z 141$^-$ from *m*-fluoronitrobenzene decreases slightly as m/z 157$^-$ and 159$^-$ from *m*-chloronitrobenzene increase. After about 150 ms, the ratio of ion abundances reaches a constant value which is indicative of equilibrium for the reaction

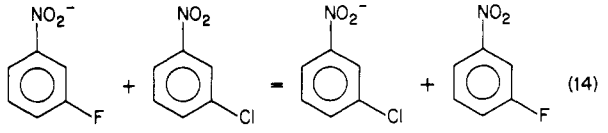

(14)

Evaluation of an equilibrium constant at 300 ms gives $K = 4.9$ for this reaction. The free energy change can be calculated by using $\Delta G° = -RT \ln K$. If we assume that the temperature of the ions and neutral molecules is 357 K, the same as the temperature of the ICR cell, the data in Figure 1 give a value of $\Delta G° = -1.1$ kcal/mol for reaction 14. The temperature of the ions cannot be measured directly, but previous work has shown that large polyatomic ions are rapidly thermalized by radiative emission, resonant charge transfer, and inelastic ion–neutral molecule collisions.[10,14–16,22]

Ion cyclotron double resonance was used to confirm that these two ions are coupled by an electron-transfer reaction. Figure 2 shows a double resonance ejection time plot for m/z 157$^-$. The upper trace is the normal time plot of ion abundance vs. reaction time. At a delay time of 260 ms, a pulsed double-resonance rf signal at the cyclotron frequency of m/z 141$^-$ ejects it from the cell and causes the m/z 157$^-$ ion signal to decay exponentially. The rapid decay of the signal for m/z 157$^-$ shows that reaction 14 is rapid, even in the endothermic direction. By analyzing the slope of the decay curve, an estimate of 2×10^{-10} cm^3/(molecule-s) was obtained for the rate constant of the reverse reaction. The rate constant for the forward reaction is just slightly smaller than the theoretical ADO rate constant of 1.5×10^{-9} cm^3/(molecule-s).[26–31]

Figure 3 shows the results of additional experiments of this same type involving various substituted benzoquinones, nitrobenzenes, and aromatic ketones. On this scale benzophenone is the one having the lowest electron affinity, and tetrachlorobenzoquinone has the highest electron affinity. The free energy differences are given in kilocalories/mole. Note that the two columns of the scale overlap with 1,4-naphthoquinone shown at the top of one and near the bottom of the other. The entire scale covers a range of 45 kcal/mol (1.95 eV). Each reported value is the average of at least three determinations of $\Delta G°$. Multiple overlaps were used to ensure internal consistency of the data. For example, the $\Delta G°$

Table I. Relative Electron Affinities Determined by the Pulsed ICR Equilibrium Method

compound	rel, electron affinity[a]
nitrobenzenes	
p-dinitrobenzene	27.7
m-dinitrobenzene	20.3
m-nitrobenzonitrile	18.5
2,7-dinitrotoluene	16.1
1,2-dichloro-4-nitrobenzene	15.9
m-nitro-α,α,α-trifluorotoluene	14.8
1,2-dichloro-3-nitrobenzene	12.4
1-chloro-3-nitrobenzene	11.7
1-chloro-4-nitrobenzene	11.0
1-fluoro-3-nitrobenzene	10.5
1-chloro-2-nitrobenzene	8.4
1-fluoro-2-nitrobenzene	8.2
1-fluoro-4-nitrobenzene	8.0
nitrobenzene	6.4
3-fluoro-6-nitrotoluene	6.0
3-nitrotoluene	5.4
N,N-dimethyl-3-nitroaniline	5.3
4-nitrotoluene	5.0
2-nitrotoluene	4.7
1,2-dimethyl-4-nitrobenzene	4.2
1,2-dimethyl-3-nitrobenzene	4.0
1,3-dimethyl-4-nitrobenzene	3.4
1,3-dimethyl-2-nitrobenzene	1.6
1,3,5-trimethyl-2-nitrobenzene	0.8
benzophenones	
4-chlorobenzophenone	3.7
4,4′-difluorobenzophenone	2.4
4-fluorobenzophenone	1.2
benzophenone	(0)
acetophenones	
2-hydroxyacetophenone	4.0
p-benzoquinones	
tetrachloro-*p*-benzoquinone	45.6
trichloro-*p*-benzoquinone	42.3
methyltrichloro-*p*-benzquinone	40.8
2,6-dichloro-bromo-*tert*-butyl-*p*-benzoquinone	39.9
2,6-dichloro-*p*-benzoquinone	39.4
tetrafluoro-*p*-benzoquinone	38.5
2,5-dichloro-*p*-benzoquinone	36.8
2,3-dichloro-*tert*-butyl-*p*-benzoquinone	35.9
2,5-dichloro-3,6-dimethyl-*p*-benzoquinone	33.5
2-chloro-5-*tert*-butyl-*p*-benzoquinone	31.6
2-chloro-5-methyl-*p*-benzoquinone	30.8
2-chloro-3,6-dimethyl-*p*-benzoquinone	28.6
chlorotrimethyl-*p*-benzoquinone	27.1
p-benzoquinone	26.3
tert-butyl-*p*-benzoquinone	25.7
methyl-*p*-benzoquinone	24.6
2,6-dimethyl-*p*-benzoquinone	22.7
trimethyl-*p*-benzoquinone	21.0
tetramethyl-*p*-benzoquinone	19.2
anhydrides	
maleic anhydride	16.0
phthalic anhydride	10.7
1,4-naphthoquinones	
1,4-naphthoquinone	23.4
2-methyl-1,4-naphthoquinone	22.0
SO_2	9.4

[a] Electron affinity relative to benzophenone (±0.2 kcal/mol)

(26) (a) Su, T.; Bowers, M. T. *J. Chem. Phys.* **1973**, *58*, 3027. (b) Su, T.; Bowers, M. T. *Int. J. Mass Spectrom. Ion Phys.* **1973**, *12*, 347. (c) *Int. J. Mass Spectrom. Ion Phys.* **1975**, *17*, 211.
(27) Lifshitz, C.; Tiernan, T. O.; Hughes, B. M. *J. Chem. Phys.* **1973**, *59*, 3182.
(28) Celotta, R. J.; Bennett, R. A.; Hall, J. L. *J. Chem. Phys.* **1974**, *60*, 1740.
(29) Kunii, T. L.; Kuroda, H. *Theor. Chim. Acta* **1968**, *11*, 97.
(30) Compton, R. N.; Reinhardt, P. W.; Cooper, C. D. *J. Chem. Phys.* **1974**, *60*, 2953.
(31) Cooper, C. D.; Naff, W. T.; Compton, R. N. *J. Chem. Phys.* **1975**, *63*, 2752.

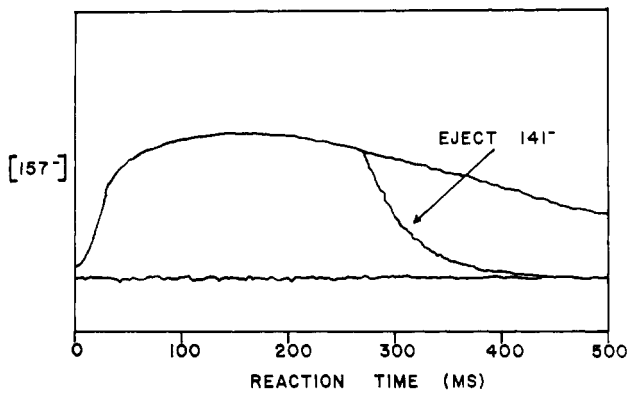

Figure 2. Ion cyclotron double-resonance ejection time plot for m/z 157⁻ with ejection of m/z 141⁻ from *m*-fluoronitrobenzene. The rapid decay of m/z 157⁻ indicates that electron transfer between the two nitrobenzenes is rapid.

from nitrobenzene to *p*-fluoronitrobenzene was determined in a direct experiment to be −1.6 kcal/mol. This value agrees well with the sum of the separate determinations for nitrobenzene to *o*-chloronitrobenzene (−2.0 kcal/mol) and *o*-chloronitrobenzene to *p*-fluoronitrobenzene (+0.3 kcal/mol). The overall consistency of the scale ±0.2 kcal/mol. These results are tabulated in Table I with benzophenone arbitrarily assigned a value of 0.0.

The molecular anions formed by electron capture were generally the only negative ions observed in the mass spectrum. However, for hindered nitrobenzenes, such as 2-nitroxylene, a $[M - 30]^-$ peak was observed in a lesser abundance than the molecular ion. This corresponds to a loss of NO to form a stable phenoxide ion. It was also observed that in molecules containing a Br or I substituent, Br^- or I^- formed via dissociative electron attachment.

The molecules shown in figure 3 can be roughly classed into two categories of reactivity. First, rapid electron transfer is observed between systems which form localized negative ions. Nitrobenzenes with electron-withdrawing substituents fall into this category. The rate constants for exothermic electron transfer are generally greater than 5×10^{-10} cm³/(molecule-s), and the cross sections for capture of electrons are also quite large. Second reactions are noticeably slower, and the electron attachment cross sections are also much smaller. This category included benzophenones and substituted nitrobenzenes with electron-releasing substituents such as methyl. Reliable equilibrium constants can be measured for these reactions with the pulsed ICR technique, but more care must be taken to avoid artifacts caused by impurities and ion losses. We have not made quantitative measurements of cross sections for attachment or rates of electron transfer, but the effects of double-resonance ejection and the ease of generation of the radical anions provide qualitative measures of these trends.

Discussion

One of the features of the equilibrium electron-transfer method is that it measures relative adiabatic electron affinities rather than vertical detachment energies. The main rationale for this assumption is that the measured rate constants agree with those expected for orbiting collisions and formation of an ion–molecule complex. Orbiting ion–molecule collisions are relatively slow processes, and there is ample time for the ion to adjust its structure to the lowest energy configuration. This is in contrast to the spectroscopic electron detachment experiments in which only Franck–Condon transitions are allowed from the potential energy surface of the ion to that of the neutral.

In another sense, however, this feature of the equilibrium method implies several limitations. Detailed information on ion and neutral structures is not available since the experiment deals with a thermal distribution of ions. In addition, care must be taken in relating the experimental $\Delta G°$ values to molecular electron affinities. Obviously the two quantities are related, but an electron affinity is defined strictly in terms of the *energy* separation of the ground-state ion and neutral.

For the general electron-transfer reaction

$$A^{-\cdot} + B = B^{-\cdot} + A \qquad (15)$$

our experimental results can be related to molecular electron affinities by using the fundamental definition of an equilibrium constant in terms of molecular partition functions. The free energy change can be written as

$$\Delta G° = -RT \ln K = \Delta E - RT \ln \left(\frac{Q_A Q_{B^-}}{Q_B Q_{A^-}} \right) \qquad (16)$$

where T is the temperature, ΔE is the energy change for the reaction at 0 K, and the Q's are molecular partition functions. ΔE, the energy separation between the ground states of the products and the reactants, is essentially the same as EA(A) − EA(B), the difference in their adiabatic electron affinities. In general the partition function term in eq 16 is expected to be small for reactions of this type since the ratio of partition functions is close to 1. This is clearly a good approximation for the translational partition functions for A⁻ and A since the mass of an electron is small compared to the mass of the molecules. In addition, since the structures of the substituted molecules and their anions are similar, differential rotational and vibrational contributions to the partition functions will be quite small. Contributions to $\Delta G°$ from the electronic partition functions are also small since there is an odd-electron anion and an even-electron molecule on both sides of the equilibrium. Thus, we conclude that the $\Delta G°$ values shown in Table I are approximately equal to their relative electron affinities.

The same conclusion can be reached by examining the fundamental definition of entropy, $S = -(\partial G/\partial T)_p$. When this is used, the entropy change for reaction 15 can be written as

$$\Delta S = R \ln \left(\frac{Q_A Q_{B^-}}{Q_B Q_{A^-}} \right) + RT \frac{\partial}{\partial T} \left(\ln \left(\frac{Q_A Q_{B^-}}{Q_B Q_{A^-}} \right) \right) \qquad (17)$$

Since the ratio of the partition functions is close to 1 and has a small temperature coefficient, ΔS is expected to be very small for these reactions.

Substituent Effects. The substituent effects on the various classes of compounds, e.g., benzophenones, nitrobenzenes, and benzoquinones, exhibit remarkable additivity. For example, this can be illustrated by comparing the electron affinity of benzophenone with both 4-fluorobenzophenone and 4,4′-difluorobenzophenone. Each 4-fluoro substituent increases the electron affinity of the parent compound by 1.2 kcal/mol.

The electron affinity of only one chloro-substituted benzophenone was measured. The 4-chloro substituent adds 3.7 kcal/mol to the electron affinity of benzophenone.

The monofluoro-substituted nitrobenzenes exhibited the following behavior:

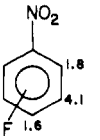

(18)

The numbers (in kilocalories/mole) corresponding to the ortho, meta, and para positions allow calculation of the appropriate isomer. For example, the electron affinity value for *o*-fluoronitrobenzene is calculated by adding 1.8 kcal/mol to the electron affinity of nitrobenzene. Subtle effects such as the greater inductive ability of the substituent at the ortho position relative to the para position are evident. The strong π donor ability of fluoro is manifested by the low value of the ortho and para substituent effect relative to the meta.

Similarly the chloro substituent effects on nitrobenzene are shown schematically:

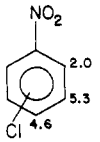

(19)

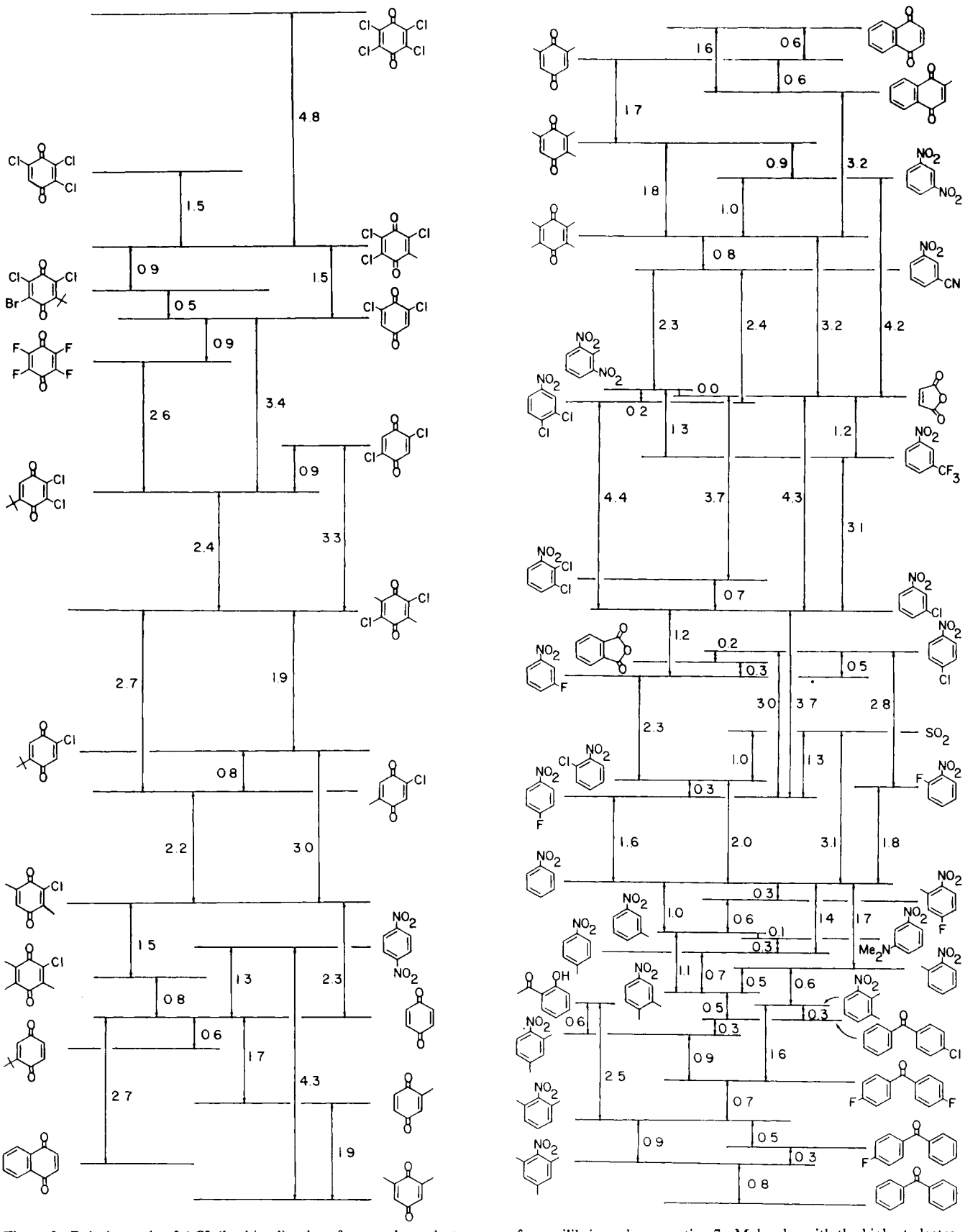

Figure 3. Relative scale of $\Delta G°$ (kcal/mol) values for gas-phase electron-transfer equilibria such as reaction 7. Molecules with the highest electron affinities are at the top left, and the lowest are at the bottom right.

The relative π donor ability of chloro is measured by comparing the para and meta values. The low ortho value is due to steric interaction of the chloro substituent with the nitro group, which is forced slightly out of plane with the phenyl ring. The compound, 1,2-dichloro-4-nitrobenzene, is predicted to have an electron affinity 9.9 kcal/mol greater than the electron affinity of nitrobenzene. The actual value (9.5 kcal/mol) is slightly lower and may reflect a saturation effect. Another dichloro isomer, 1,2-dichloro-3-nitrobenzene, is predicted to have a value (7.3 kcal/mol) much different than is observed (6.0 kcal/mol). This can be

attributed to the unfavorable $\pi-\pi$ interaction of the two chloro substituents.

The methyl substituent effects on nitrobenzenes are illustrated below:

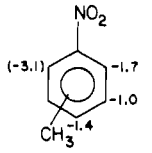

(20)

The destabilizing effect of methyl is due to its weak π and σ donor ability. The greater destabilizing ability of the ortho vs. para position is due to the unfavorable steric effect of the ortho isomer. The predicted electron affinity of 1,2-dimethyl-4-nitrobenzene (−2.4 kcal/mol) is close to the measured value (−2.2 kcal/mol). Similarly the electron affinity of 1,3-dimethyl-4-nitrobenzene is accurately predicted. However the predicted value of 1,3-dimethyl-2-nitrobenzene (−3.4 kcal/mol) is in error by 1.4 kcal/mol. This is due to the two *o*-methyl groups forcing the nitro group out of plane to a much greater degree than predicted on the basis of additivity. The second *o*-methyl substituent effect is shown above in parentheses (−3.1). The trisubstituted (1,3,5-trimethyl-4-nitrobenzene) compound is predicted to have a value of −6.2 kcal/mol. This differs from the actual value (−5.8 kcal/mol) due to a saturation effect.

The benzoquinones exhibit no saturation for the methyl-substituted compounds:

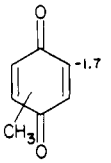

(21)

The mono-, di-, tri-, and tetramethyl-substituted compounds are separated by about −1.7 kcal/mol, the same as the *o*-methyl effect in nitrobenzene.

Chloro substituent effects for the benzoquinones are slightly more complicated. A single chloro substituent increases the electron affinity by about 6.2 kcal/mol, but for benzoquinones with two or more chloro substituents situated ortho or para to each other the increase is only about 5.25 kcal/mol. For example, when these values are used, 7.1 kcal/mol is predicted for 2,5-dichloro-3,6-dimethyl-*p*-benzoquinone (plus 5.25 for each chlorine substituent and minus 1.7 for each methyl substituent). This is very close to the measured value of 7.2 kcal/mol.

Figure 4 shows how the relative electron affinities determined by the pulsed ICR equilibrium electron-transfer method compare with those determined by various other methods such as photoelectron spectroscopy, collisional ionization, and electron charge transfer. It is apparent that the relative ICR electron affinity values have a much smaller uncertainty (±0.01 eV) than the electron charge transfer and collisional ionization values (compounds **1** and **4**–**7**). Generally the relative order of electron affinities is the same. One exception is that the pulsed ICR data suggest that the electron affinity of chloranil is greater than that for fluoranil. This is consistent with the substituent effects in the benzophenone and nitrobenzene series but is opposite to the order obtained by electron charge transfer experiments.[32]

We recently reported a much higher electron affinity for SO_2 (2.2 eV) than had been previously accepted (1.1 eV).[9] Our measurement has been called into question by recent flowing afterglow results[33] and high-pressure mass spectroscopy experiments.[34] Figure 4 supports the lower value for EA(SO_2), but

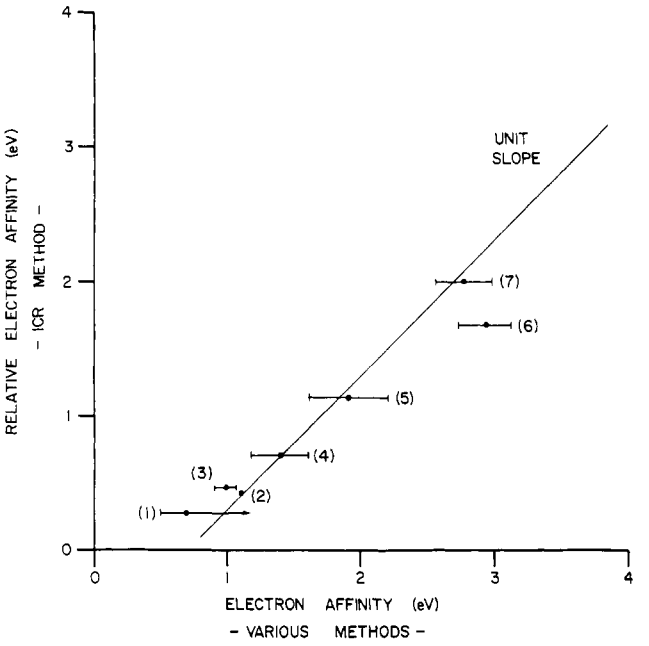

Figure 4. Comparison of relative electron affinities determined by the pulsed ICR equilibrium method with absolute EA's measured by various other methods: (1) nitrobenzene;[27] (2) SO_2;[28] (3) phthalic anhydride;[29] (4) maleic anhydride;[30] (5) benzoquinone;[31] (6) fluoranil;[32] (7) chloranil.[32]

at this time we have not determined the nature of the error, if any, in our prior work with SO_2. It is important to note that the *relative* electron affinities measured by pulsed ICR and high-pressure mass spectrometry agree well.

Acknowledgment. We gratefully acknowledge research support from the National Science Foundation and the donors of the Petroleum Research Fund, administered by the American Chemical Society. We also acknowledge some early work on the electron affinity scale by Steven R. Masuda. We thank Prof. Harold Moore for kindly providing the substituted benzoquinones.

Registry No. *p*-Dinitrobenzene, 100-25-4; *m*-dinitrobenzene, 99-65-0; *m*-nitrobenzonitrile, 619-24-9; 2,6-dinitrotoluene, 606-20-2; 1,2-dichloro-4-nitrobenzene, 99-54-7; *m*-nitro-α,α,α-trifluorotoluene, 98-46-4; 1,2-dichloro-3-nitrobenzene, 3209-22-1; 1-chloro-3-nitrobenzene, 121-73-3; 1-chloro-4-nitrobenzene, 100-00-5; 1-fluoro-3-nitrobenzene, 402-67-5; 1-chloro-2-nitrobenzene, 88-73-3; 1-fluoro-2-nitrobenzene, 1493-27-2; 1-fluoro-4-nitrobenzene, 350-46-9; nitrobenzene, 98-95-3; 3-fluoro-6-nitrotoluene, 446-33-3; 3-nitrotoluene, 99-08-1; *N,N*-dimethyl-3-nitroaniline, 619-31-8; 4-nitrotoluene, 99-99-0; 2-nitrotoluene, 88-72-2; 1,2-dimethyl-4-nitrobenzene, 99-51-4; 1,2-dimethyl-3-nitrobenzene, 83-41-0; 1,3-dimethyl-4-nitrobenzene, 89-87-2; 1,3-dimethyl-2-nitrobenzene, 81-20-9; 1,3,5-trimethyl-2-nitrobenzene, 603-71-4; 4-chlorobenzophenone, 134-85-0; 4,4′-difluorobenzophenone, 345-92-6; 4-fluorobenzophenone, 345-83-5; benzophenone, 119-61-9; 2′-hydroxyacetophenone, 118-93-4; tetrachloro-*p*-benzoquinone, 118-75-2; trichloro-*p*-benzoquinone, 634-85-5; methyltrichloro-*p*-benzoquinone, 4592-97-6; 2,6-dichlorobromo-*tert*-butyl-*p*-benzoquinone, 94905-00-7; 2,6-dichloro-*p*-benzoquinone, 697-91-6; tetrafluoro-*p*-benzoquinone, 527-21-9; 2,5-dichloro-*p*-benzoquinone, 615-93-0; 2,3-dichloro-*tert*-butyl-*p*-benzoquinone, 34403-14-0; 2,5-dichloro-3,6-dimethyl-*p*-benzoquinone, 46010-98-4; 2-chloro-5-*tert*-butyl-*p*-benzoquinone, 94905-01-8; 2-chloro-5-methyl-*p*-benzoquinone, 19832-87-2; 2-chloro-3,6-dimethyl-*p*-benzoquinone, 40853-39-2; chlorotrimethyl-*p*-benzoquinone, 51028-70-7; *p*-benzoquinone, 106-51-4; *tert*-butyl-*p*-benzoquinone, 3602-55-9; methyl-*p*-benzoquinone, 553-97-9; 2,6-dimethyl-*p*-benzoquinone, 527-61-7; trimethyl-*p*-benzoquinone, 935-92-2; tetramethyl-*p*-benzoquinone, 527-17-3; maleic anhydride, 108-31-6; phthalic anhydride, 85-44-9; 1,4-naphthoquinone, 130-15-4; 2-methyl-1,4-naphthoquinone, 58-27-5; sulfur dioxide, 7446-09-5.

(32) Cooper, C. D.; Frey, W. F.; Compton, R. N. *J. Chem. Phys.* **1978**, *69*, 2367.
(33) Grabowski, J. J.; Van Doren, J. M.; DePuy, C. H.; Bierbaum, V. H. *J. Chem. Phys.* **1984**, *80*, 575.
(34) Caldwell, G.; Kebarle, P. *J. Chem. Phys.* **1984**, *80*, 577.